



Effect of Annealing Temperature on the Structural Properties of Dual Solution Synthesized AIS: ZnS Thin Films



Akwuegbu, C. O.¹, Nwaokorongwu, E. C.^{1*}, Okpechi, K. U. P.¹, Joseph, U.¹ and Emea, A. E.²

¹Department of Physics, Michael Okpara University of Agriculture, Umudike, PMB 7267 Umuahia, Abia State, Nigeria.

²Department of Physics Clifford University Owerri, Abia State, Nigeria.

*Corresponding Author Email: nwaokorongwu.elizabeth@mouau.edu.ng Phone: +2347061238732

ABSTRACT

Using two solution-based techniques—solution growth technique (SGT) and sequential ionic layer adsorption and reaction (SILAR) AIS: ZnS alloyed thin films were successfully produced on glass substrates. The sources of Al, Zn, and S were aluminum sulphate (AlSO₄·7H₂O), zinc sulphate (ZnSO₄·7H₂O), and sodium thiosulphate (Na₂S₂O₃). The complexing agent that was utilized was ethylene diamine tetraacetic acid (EDTA). Using a Master Chef Annealing Machine, the deposited alloyed samples were annealed between 373K and 523K. The scanning electron microscope (SEM) and X-ray diffractometer (XRD) were used for the crystallographic investigations. Samples R1 and R6 AIS: ZnS alloyed thin films exhibit well-defined peaks in their XRD pattern, indicating that they are polycrystalline in nature. We computed their grain sizes. Spectroscopy using Rutherford backscattering (RBS). Analysis using Rutherford backscattering spectroscopy (RBS) verified the composition of aluminum, zinc, and sulfur in the alloyed thin films. The microstructure of the deposited alloyed thin films is revealed by the results of surface electron microscopy. Two significant semiconductor materials that have potential uses in optoelectronics, photovoltaics, and sensing devices are aluminum sulfide (AIS) and zinc sulfide (ZnS). Depositing these materials in thin films at a reasonable cost and with good efficiency is possible with dual solution synthesis. However, the annealing temperature, a crucial factor in establishing the crystal structure, morphology, and optical properties of these films, can have an impact on their structural characteristics. Prior studies have examined how the annealing temperature affects the structural characteristics of AIS and ZnS thin films separately; however, the dual solution-produced AIS: ZnS thin films have not received as much attention. The purpose of this work is to examine how the annealing temperature affects the crystal structure and surface morphology of AIS: ZnS thin films. The results of this investigation can offer significant understanding regarding the refinement of the annealing temperature to produce superior AIS: ZnS thin films for a range of uses. Based on their properties, sulphide alloyed thin films could find applications in microelectronics, window coating, and antireflection coating. They work well as coatings for eyeglasses and as absorber layers for photocells, among other applications.

Keywords:

Annealing,
Dual solution synthesis,
Thin films,
AIS:ZnS.

INTRODUCTION

Thin film deposition techniques have made significant strides possible in a variety of technical applications recently, including electroluminescent displays, solar cells, laser diodes, and others. Because ZnS is highly toxic, its main advantages include thin-film coating in optical and microelectronics and the ability to replace CdS (2.4 eV), which has a wider band gap, with ZnS (3.7

eV) as a buffer layer to improve the cells' short-circuit current and decrease window absorption losses (Kumar et al., 2016a). Since un-doped ZnS films have a very high electrical resistivity (usually 10⁷ Ωcm), the electrical resistivity must be reduced to achieve its full conductivity behavior. This can be accomplished by doping these layers with appropriate impurity atoms without

significantly altering the layers' optical characteristics (Eid et al., 2010).

There are various varieties of aluminum sulphide (AlS), which has a crystal structure resembling that of wurtzite. According to Hossain et al. (2019), thin films of aluminum sulphide have several uses in the electronic industry, including optoelectronics and solar cell manufacturing. Specialized materials with remarkable electrical, optical, and structural capabilities are aluminum sulphides. Numerous technologies, such as heterogeneous catalysts, energy conversion and storage devices, transistors, photodetectors, and gas sensors, have included aluminum sulphides.

One of the direct-VI semiconductor compounds, zinc sulphide (ZnS), has a significant band gap energy of about 3.65 eV at ambient temperature. The substance is used as a reference material to test several theoretical models in condensed matter physics and crystallizes in both cubic and hexagonal forms (Altaf, 2015). According to Elidrisset al. (2019), the material has a wide range of potential uses in photovoltaic and optoelectronic devices, both in bulk and thin film forms. It serves as the primary component of solar control coatings, optoelectronics, electroluminescence, sensors, and other devices.

Because of its wide band gap, which lowers window absorption losses and increases the cell's short circuit current, ZnS thin film is primarily used as a window layer in heterojunction photovoltaic solar cells (Kumar et al., 2005). ZnS is transparent to visible light and opaque to ultraviolet and near-infrared radiation, according to research (Osiele in Oluwatoyin, 2020). According to Oladji and Chow (2005), ZnS materials may also be utilized in radio frequency field-sputtered films like CdZnS and modified ZnS/CdS. ZnS thin films have been fabricated using a variety of methods, including sputtering (Shao et al., 2020), molecular beam epitaxy (Kavanagh and Cameron, 2011), spray pyrolysis (Elidrisset al., 2015), pulsed-laser deposition (Yano et al., 2020), chemical bath deposition (Fukarova-Juruskovska et al., 2020), chemical vapour deposition (Kashani in Oluwatoyin, 2020), liquid phase atomic layer epitaxy (Lindroos et al., 2020), and spin coating (Kumar et al., 2015). Among them, the spin coating process is a desirable thin-film deposition method due to several factors, including its rapid operating system, ease of scaling up, less risk, and increasing uniformity as it thins. Furthermore, the films grow at a reasonably low temperature, which makes them suitable with flexible organic substrates. Therefore, it may be combined with advanced silicon technologies without requiring the usage of metal catalysts. To further efficiently control the morphologies and qualities of the final product, a variety of parameters (such as acceleration, fume exhaust, time of spin, and spin speed) can be changed (Tyona, 2013). In this work, a straightforward dual solution approach was used to deposit AlS-doped ZnS films. This approach,

which is supposed to dope the films consistently, worked well. Nonetheless, the goal of this work is to comprehend how the annealing temperature affects the development and characterization of AlS: ZnS thin films.

MATERIALS AND METHODS

Preparation of AlS: ZnS alloy thin films

Substrate preparation

In this work, AlS-doped ZnS films were deposited using a simple dual solution method. This method, which aims to constantly dope the movies, performed admirably. However, the objective of this work is to understand the effects of the annealing temperature on the growth and characterization of AlS: ZnS thin films.

Deposition of sulphide alloy thin films using dual solution synthesis (SGT AND CBD)

Compounds were deposited in this study utilizing the SILAR method and solution growth. After utilizing SILAR to create thin layers of aluminum sulfide alloy (AlS, ZnS), the samples were immersed in a solution-grown ZnS bath. By combining the two methods, four fundamental thin film layers with different annealing temperatures were ultimately produced.

Characterization of deposited thin films

The GBC Enhanced Mini Material Analyzer (EMMA) X-ray diffractometer was used to do the XRD analysis. The XRD pattern provides details about the composition and structure of the alloyed thin films of AlS: ZnS. Debye-Scherrer's equation, represented as equation 1, is used to derive the crystallite sizes listed in Table 1 (Onwumeka and Ekpunobi, 2018; Osuwa and Anusionwu, 2011; Offiah et al., 2012; Nwaokorongwu et al., 2018).

(1) where θ is Bragg's diffraction angle, λ is the wavelength of $\text{CuK}\alpha$ radiation used ($\lambda = 1.54\text{\AA} \geq 0.154\text{nm}$), λ is the grain size or average crystallite size, β is the experimentally observed diffraction peak with width at half maximum intensity (Full Width at Half Maximum, or FWHM), and k is the shape factor ($k=0.9$). A technique called X-ray diffraction is used to ascertain the atomic and molecular structure of crystals. The crystalline atoms in a crystal cause an incident X-ray beam to diffract into numerous distinct directions. A three-dimensional image of the electron density inside the crystal can be created by a crystallographer by determining the angles and intensities of these diffracted beams. A crystal is placed on a goniometer and slowly rotated while being exposed to X-rays to produce an X-ray diffraction pattern made up of spots that are regularly spaced and referred to as reflections. Each scatterer reradiates a small amount of its intensity as a spherical wave in response to the incoming beam, which is coming from the upper left.

These spherical waves will only be in sync (add constructively) in directions where their path-length

difference $2d \sin \theta$ equals an integer multiple of the wavelength λ if scatterers are distributed symmetrically with a separation of d . That is, $n\lambda = 2d \sin \theta$

In that instance, a reflection spot appears in the diffraction pattern as a result of a portion of the incoming beam being deflected by an angle of 2θ . Here, n is any integer, μ is the beam's wavelength, d is the distance between diffracting planes, and θ is the incident angle.

X-ray diffraction (XRD) is a non-destructive method best utilized for measuring the average distance between rows or layers of atoms, orienting a single crystal or grain, identifying the crystal structure of an unknown material, and assessing the size, shape, and internal stress of small crystalline regions. A surface electron microscope was used to analyze the SnS: ZnS thin film microstructure. One kind of electron microscopy is the scanning electron microscope (SEM). At the surface of solid specimens, it produces a range of signals using a concentrated stream

of high-energy electrons. Information about the sample, including its exterior morphology (texture), chemical composition, and the orientation and crystalline structure of the components that make up the sample, can be found in the signals that result from electron-sample RHK interactions. Since x-rays produced by electron interactions do not cause volume loss of the sample, SEM examination is regarded as "non-destructive," meaning that the same materials can be analyzed more than once (Mgbaja, 2014).

Rutherford backscattering spectroscopy (RBS) was used to establish the samples' elemental compositions and thicknesses.

RESULTS AND DISCUSSION

Table 1 shows the identification of samples of AlS: ZnS thin films with variations in annealing temperature.

Table 1: Identification of samples of AlS: ZnS thin films with variations in annealing temperature

Bath sample	Annealing temperature (K)
R0	As grown sample
R2	373
R3	423
R4	532
R5	473

Composition and Thickness Characterizations

In this study, elemental compositions and the thicknesses of the samples were determined using RBS.

The analysis also shows that samples R3, R4, and R5 expected to be CdS: ZnS thin films annealed at 423k, 523k, and 473k respectively have 25.10% aluminium, 17.52% of Zinc, 6.89% of sulphur with a thickness of

140nm, 29.84% of aluminum, 5.04% of Zinc, 6.48% of sulphur with a thickness of 171nm and 16.25% of aluminum, 9.07% of zinc, 16.04% of sulphur with a thickness of 300nm. These are shown in Figure 1, Figure 2, and Figure 3 and summarized in Table 2, Table 3, and Table 4 respectively.

Table 2: The elements in sample R3 of AlS: ZnS

Elements	Layer 1 % Composition	Layer 2 % Composition
Cd		
Si		23.74
Al	25.10	0.02
Zn	17.62	
O		63.42
K		0.69
S	16.89	
Na		8.91
Fe		0.59
Ca		2.63

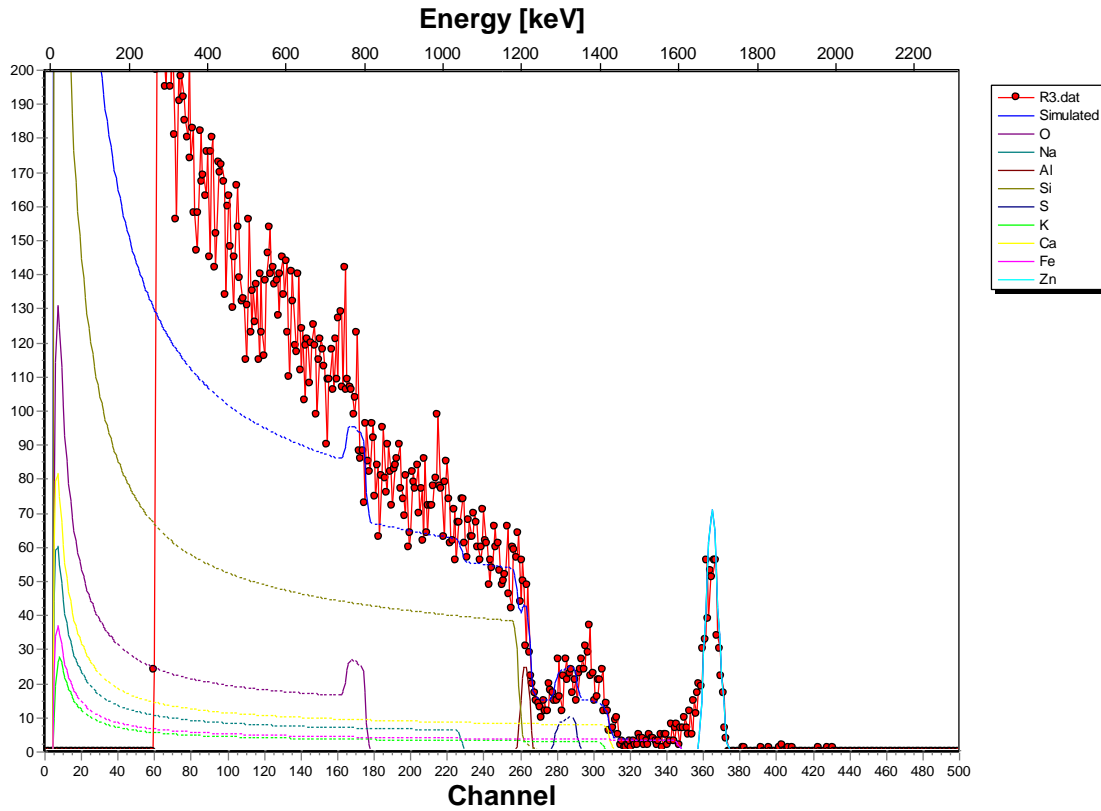


Figure 1: The composition of sample R3 with a thickness 140nm, of AlS: ZnS measured by RBS

Table 3: The elements in sample R4 of AlS: ZnS

Elements	Layer 1 % Composition	Layer 2 % Composition
Cd		
Si		23.74
Al	29.84	0.02
Zn	5.04	
O		63.42
K		0.69
S	6.48	
Na		8.91
Fe		0.59
Ca		2.63

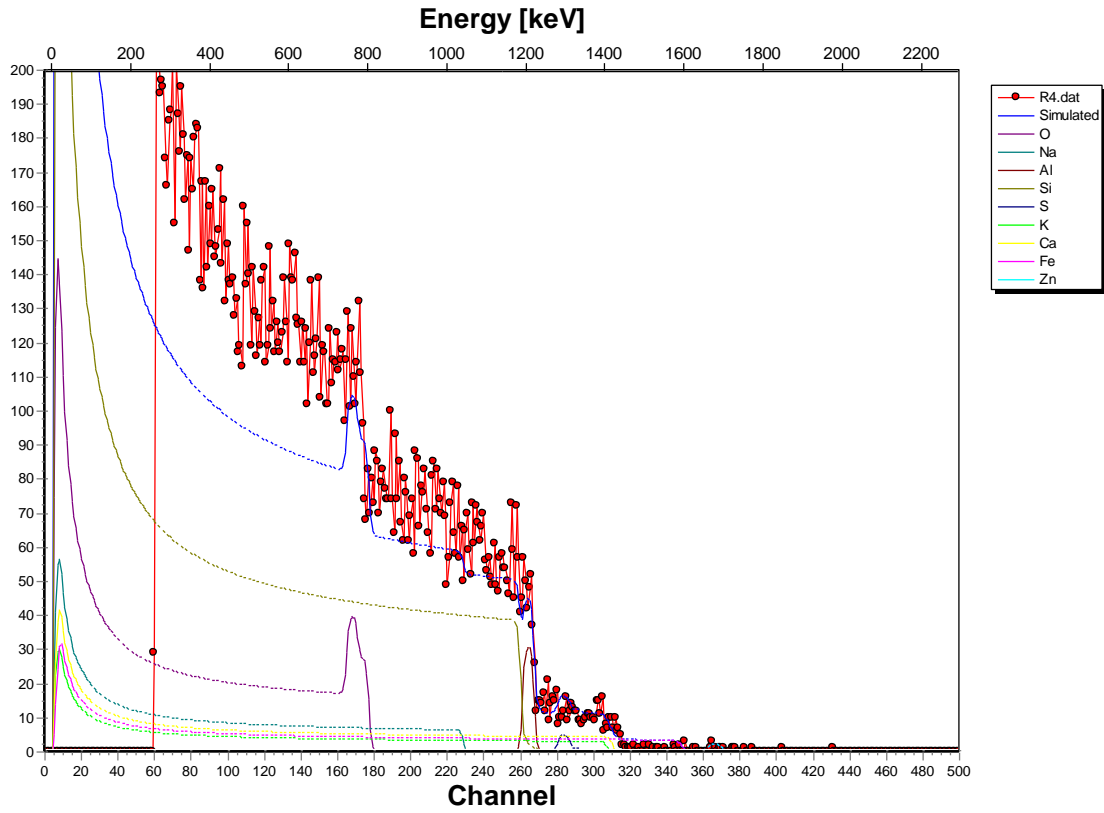


Figure 2: The composition of sample R4 with a thickness 171nm, of AlS: ZnS measured by RBS

Table 4: The elements in sample R5 of AlS: ZnS

Elements	Layer 1 % Composition	Layer 2 % Composition
Cd		
Si		23.74
Al	16.25	0.02
Zn	9.07	
O		63.42
K		0.69
S	16.04	
Na		8.91
Fe		0.59
Ca		2.63

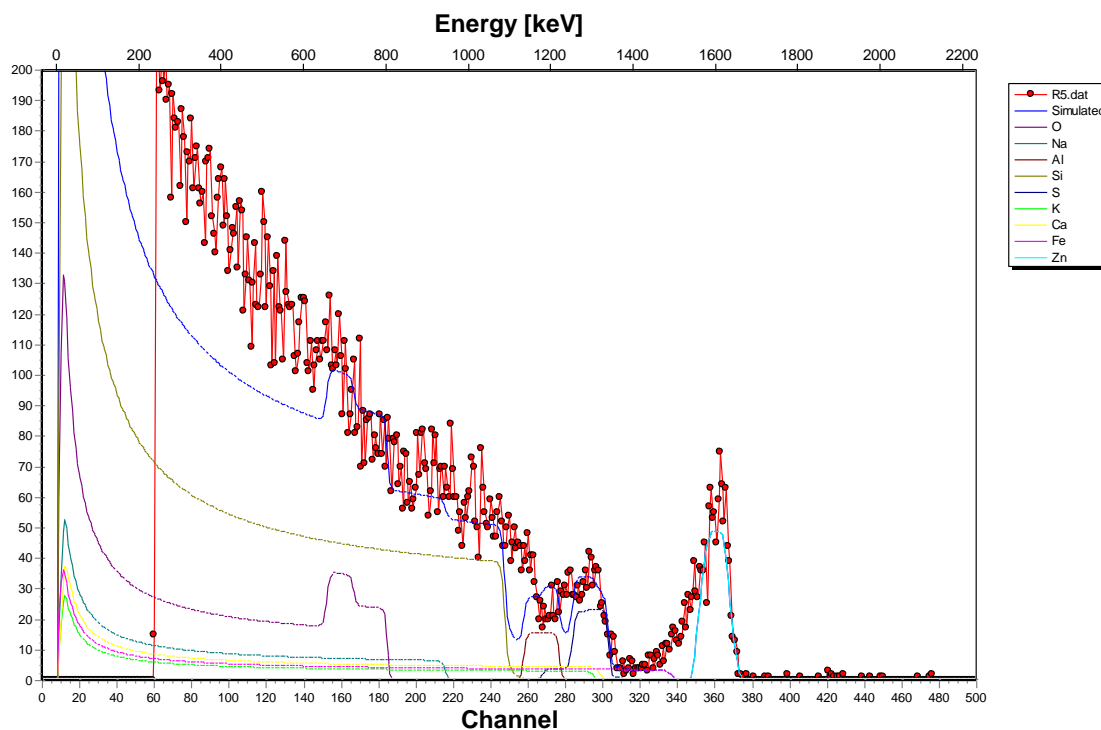


Figure 3: The composition of sample R5 with a thickness 300nm, of AlS: ZnS measured by RBS

Structural Characterization

Investigating the materials' structure is crucial. This includes utilizing XRD to determine the materials' crystallographic structure and SEM to determine the microstructure of the deposited samples.

Crystallographic Studies of the Deposited Samples

An X-ray diffractometer was used to perform the XRD analysis. The alloyed sulphide thin films of AlS: ZnS that were annealed at various temperatures are shown by the XRD pattern. Figure 4 displays the x-ray diffraction of the thin films of the sulphide alloys mentioned previously.

The crystalline character of AlS: ZnS alloys is indicated by the XRD patterns, which have crisp, well-defined peaks.

Debye-Scherrer's equation is used to get the crystallite sizes that are provided (Reka et al, 2014).

$D = k\lambda/\beta\cos\theta \sim \sim 3$ where θ is the Bragg's diffraction angle, λ is the wavelength of $\text{CuK}\alpha$ radiation used ($\lambda = 1.54\text{\AA} \geq 0.154\text{nm}$), μ is the shape factor ($k=0.9$), D is the grain size or average crystallite size, and β is the experimentally observed diffraction peak with width at half maximum intensity (Full Width at Half Maximum, or FWHM).

The XRD Pattern of AlS: ZnS Alloyed Thin Films of Samples R1 and R6

The XRD pattern of AlS: ZnS alloy thin films shows well-defined peaks which indicates the polycrystalline nature of the alloyed thin films.

Table 5: XRD results of AlS: ZnS alloyed thin film

Sample	hkl	d-spacing (Å)	FWHM (radian)	Grain size (nm)	Position($^{\circ}2\theta$)	Count (height)
R1 (AlS: ZnS annealed at 200°C)	002	9.36913	0.1279	1.5332	09	21196.46
	200	8.44092	0.0769	1.8118	11	2855.20
	020	5.74060	0.1535	0.9112	15	868.59
	111	4.67202	0.1023	1.375	19	7193.44
	202	4.24530	0.1791	0.7871	21	10060.71
R6 (AlS: ZnS annealed at 250°C)	002	11.8653	0.8187	1.3669	13	1766.70
	200	3.62251	0.2558	0.5551	24	1735.26
	020	2.95542	0.1023	1.4028	30	1032.06
	111	2.48477	0.2047	0.7122	35	512.65
	202	2.34644	0.2558	0.5732	37.5	920.99

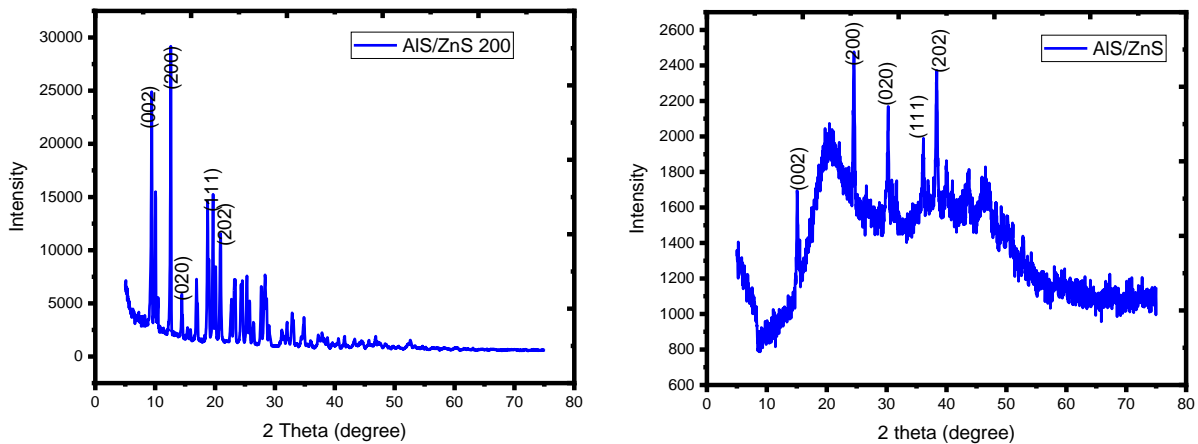


Figure 4: XRD pattern of AIS: ZnS alloyed thin films of samples R1 and R6 annealed at 200°C and 250°C respectively

Microstructure of the Deposited Samples

The microstructure of the thin films of AIS: ZnS was determined using a surface electron microscope. The process of analysis is through imaging.

Samples R1 and R6 of AIS: ZnS have smooth surfaces with no cracks and are well-defined coated thin films as shown in Fig 5.

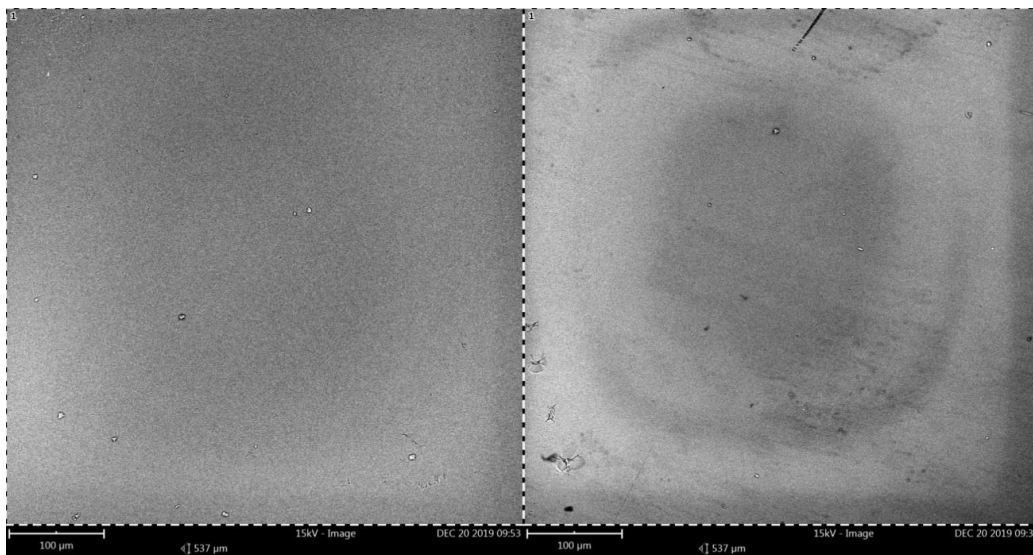


Figure 5: Optical micrograph of AIS: ZnS alloyed thin films of samples R1 and R6

CONCLUSION

Materials that were alloyed were deposited. The materials that were deposited adhered to the substrates uniformly. The number of cycles, the length of the dip, and the annealing temperature all affect how thick the materials are deposited. The deposited samples exhibit varying percentages of the desired components, as indicated by the elemental compositions. The structural characteristics indicate the polycrystalline nature of AIS: ZnS.

REFERENCES

Altaf, H. S. (2015). Irradiation effects on Nd and W doped Aluminum Nitride thin films. *Physica B Condensed Matter*, 2, 1, pp. 1-10.

Eid, A. H., Salim, S. M., Sedik, M. B., Omar, H., Dahy, T. & Abou-Elkhair, H. M. (2010). Preparation and characterization of ZnS thin films. *J. Appl. Sci. Res.* 6, 6, pp. 777-784.

Elidrissi, B., Addou, M., Regragui, M., Kachouane, A. & Bernede, J. C. (2019). Structure, composition, and optical properties of ZnS thin films prepared by spray pyrolysis. *Mater. Chem. Phys.*, 68, pp. 175-179.

Elidrissi, B., Addou, M., Regragui, M., Bougrine, A., Kachouane, A. & Bernede, J.C. (2015). Structure, composition and optical properties of ZnS thin films

- prepared by spray pyrolysis', *Math. Chem. Phys.* 68, pp. 175-179 4.
- Ezema, F. I., Asogwa, P. U., Ekwealor, A. B. C., Ugwuoke, P. E. & Osuji, R.U. (2017). Growth and optical properties of Ag₂S thin films deposited by the chemical bath deposition technique. *J. Univ. Chem. Techn. Metall.* 42, 2, pp. 217-111.
- Fukarova-Juruskovska, M., Ristov, M. & Andonovski, A. (1997). Electroluminescent cell prepared by chemical deposition of ZnS: Mn thin film. *Thin Solid Films*, 299, 2, 1, 2, pp. 149-151.
- Hossain, M., Siddiquee, K., Islam, O., Gafur, M., Qadir, M. & Ahmed N. (2019). Characterization of electrodeposited ZnTe thin films. *J. Optics* 48, pp. 95–301.
- Kashani, H. (1996). Production and evaluation of ZnS thin films by the MOCVD technique as alpha-particle detectors. *Thin Solid Films* 288, pp.50-56.
- Kumar V, Saroja M, Venkatachalam M & Shankar S 2015 Synthesis and characterization of ZnS thin films by sol-gel dip and spin coating methods. *Int. J. Rec. Sci. Res.* 6, 11, pp. 7377-7379.
- Kumar, D. S., Kumar, B. J. & Mahesh, M. M. (2018). Chapter 3 - Quantum Nanostructures (QDs): An Overview, Editor(s): Sneha Mohan Bhagyaraj, Oluwatobi Samuel Oluwafemi, Nandakumar Kalarikkal, Sabu Thomas. In *Micro and Nano Technologies, Synthesis of Inorganic Nanomaterials*, Woodhead Publishing, pp.59-88, <https://doi.org/10.1016/B978-0-08-101975-7.00003-8>.
- Kumar, R., Rathore, D. K., Meena, B. S., Ashutosh, L., Singh, M., Kumar, U. & Meena, V. K. (2016). Enhancing productivity and quality of fodder maize through soil and foliar zinc nutrition. *Indian Journal of Agriculture Research*, 50, pp. 259–63.
- Lindroos, S., Kannianen, T. & Leskela, M. (2016). Growth of ZnS thin films by liquid-phase atomic layer epitaxy (LPALE). *Appl. Surf. Sci.* 75, pp. 70-74.
- Nicolau, Y. F. (1985). Solution deposition of thin solid compound films by a successive ionic layer adsorption and reaction process. *Appl. Surf. Sci.*, 22, 23, pp. 1061-1074.
- Nwaokorongwu, E. C, Akpu, N. I. & Joseph, U. I. (2018). Growth and Optical Characterization of copper sulphide thin films by sol-gel technique. *International Journal of Innovative Scientific & Engineering Technologies Research*, 6, 2, pp. 38-44.
- Offiah, S. U., Ugwoke, P. E., Ekwealor, A.B.C., Ezugwu, S.C., Osuji, R.U. & Ezema, F.I. (2012). Structural and Spectral Analysis of Chemical Bath Deposited Copper Sulfide Thin Films for Solar Energy Conversions. *Digest Journal of Nanomaterials and Biostructures*, 7, 1, pp. 165 – 173.
- Oladeji, I. O. & Chow, L. (2005). Synthesis and processing of CdS/ZnS multilayer films for solar cell application. *Thin Solid Films*, 474, pp. 77-83.
- Oluwatoyin, O. (2020). Preparation and Characterization of ZnS Thin Films Grown by Spin Coating Technique. *Tanzania Journal of Science*, 46, 2, pp. 534-547.
- Onwuemeka, J. J. & Ekpunobi, A. J. (2018). Synthesis of CdO: SnO₂ Alloyed Thin Films for solar energy conversion and Optoelectronic Application. *Springer-Journal of Material Science; Materials in Electronics*. 29, pp. 9176-9183.
- Osiele, O. M. (2001). Chemically Deposited ZnS thin film for solar energy applications. *J. Appl. Sci.* 4, 1, pp. 1690-1699.
- Osuwa, J. C. & Anusionwu, P.C. (2011). Some Advances and prospects in nanotechnology: A Review. *Asian Journal of Information Technology*, 10, pp. 96-100.
- Osuwa, J. C & Mgbaja E. C. (2014). Structural electrical properties of copper sulphide (CuS) thin films doped with mercury and nickel impurities. *IOSR Journal of Applied Physics* 6 (5), 28-31.
- Shao, L. X., Chang, K. H. and Hwang, H. L. (2003) Zinc sulfide thin films deposited by RF reactive sputtering for photovoltaic applications. *Appl. Surf. Sci.* 212, 213, pp. 305-310.
- Tyona, M. D. (2013). A theoretical study on spin coating technique. *Adv. Mater. Res.* 2, 4, pp. 195-208.
- Yano, S., Schroeder, R., Ullrich, B. & Sakai, H. (2003). Absorption and photocurrent properties of thin ZnS films formed by pulsed-laser deposition on quartz. *Thin Solid Films*, 423, pp. 273-276. S0040-6090Z02.010